CMB lensing – radio galaxy cross-correlation

Rupert Allison
University of Oxford
6^{th} July 2015

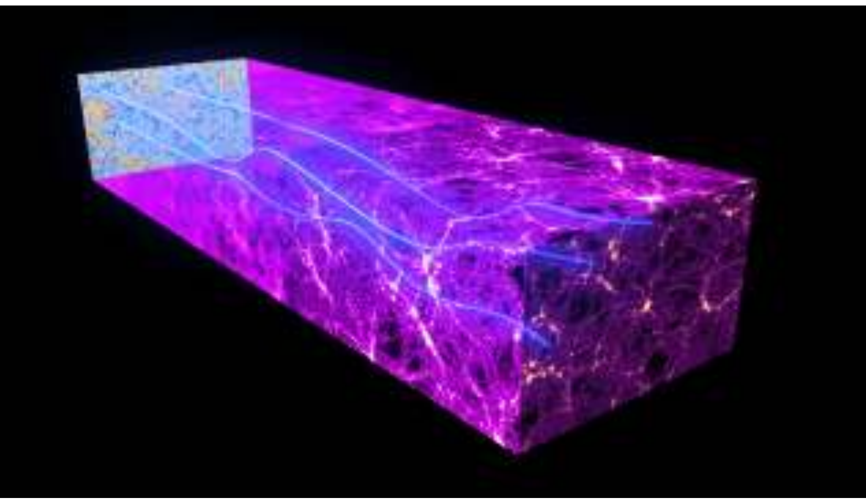 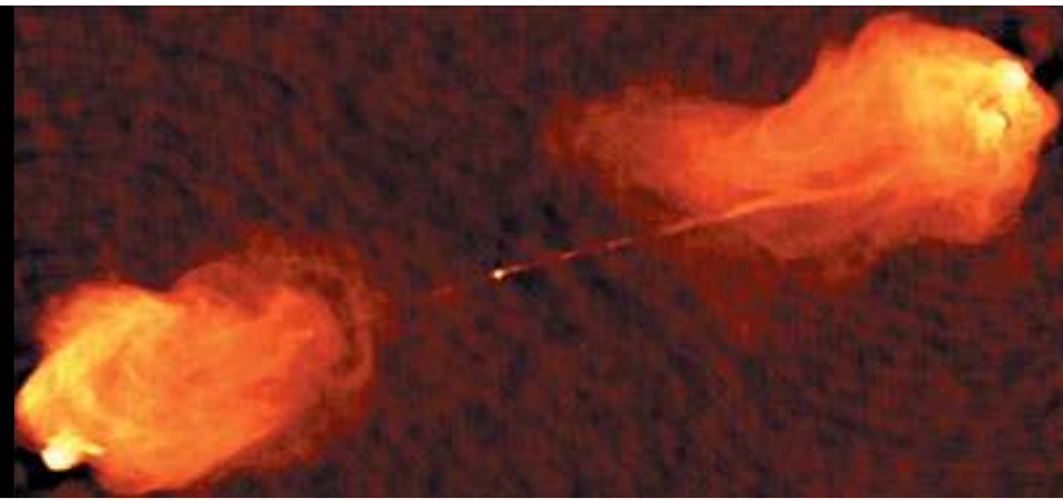

arXiv: **1502.06456**

Collaborators: Sam Lindsay, Blake Sherwin, Matt Jarvis, ACT Collaboration

Outline

- **Motivation**, science to extract
- **Physics of cross-correlation**
- **CMB lensing** from ACT and ACTPol
- **FIRST radio survey**: AGN sample
- **Results** and future prospects

Motivation

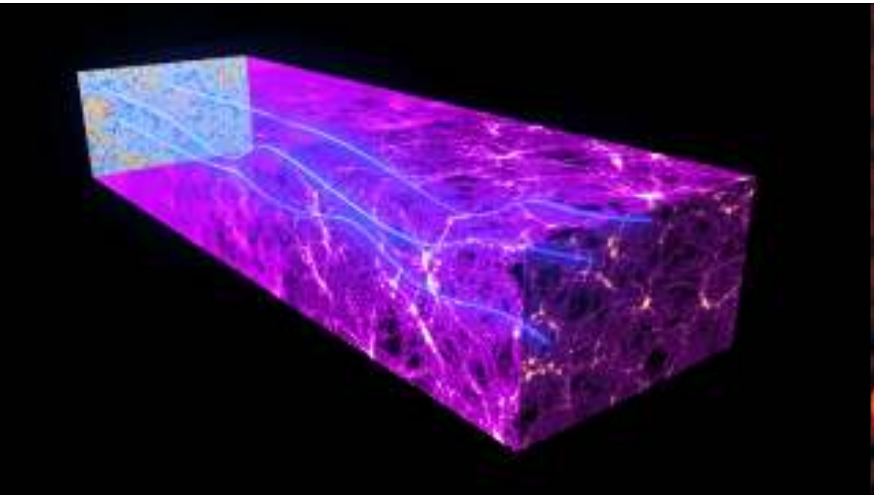

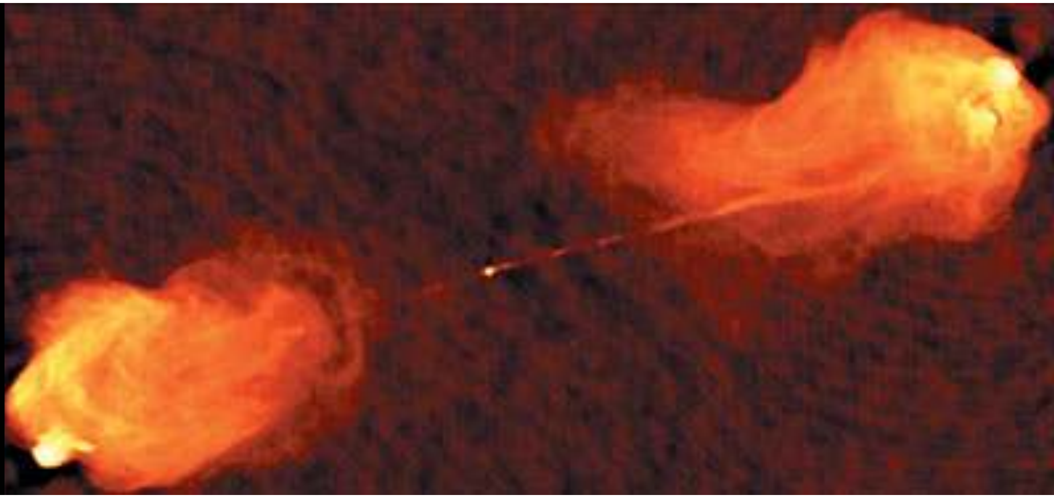

CMB lensing – radio galaxy cross-correlation

- Excellent overlap between source kernels
- Constrain the bias of AGN
- Calibration of auto-correlation, extraction of cosmology
- Characterize mass of the AGN haloes
- Multi-tracer technique
- Robust to systematics

Physics of lensing-galaxy correlation

- Radio galaxies are biased tracers of the underlying dark matter density field
- CMB lensing also due to density fluctuations of the dark matter

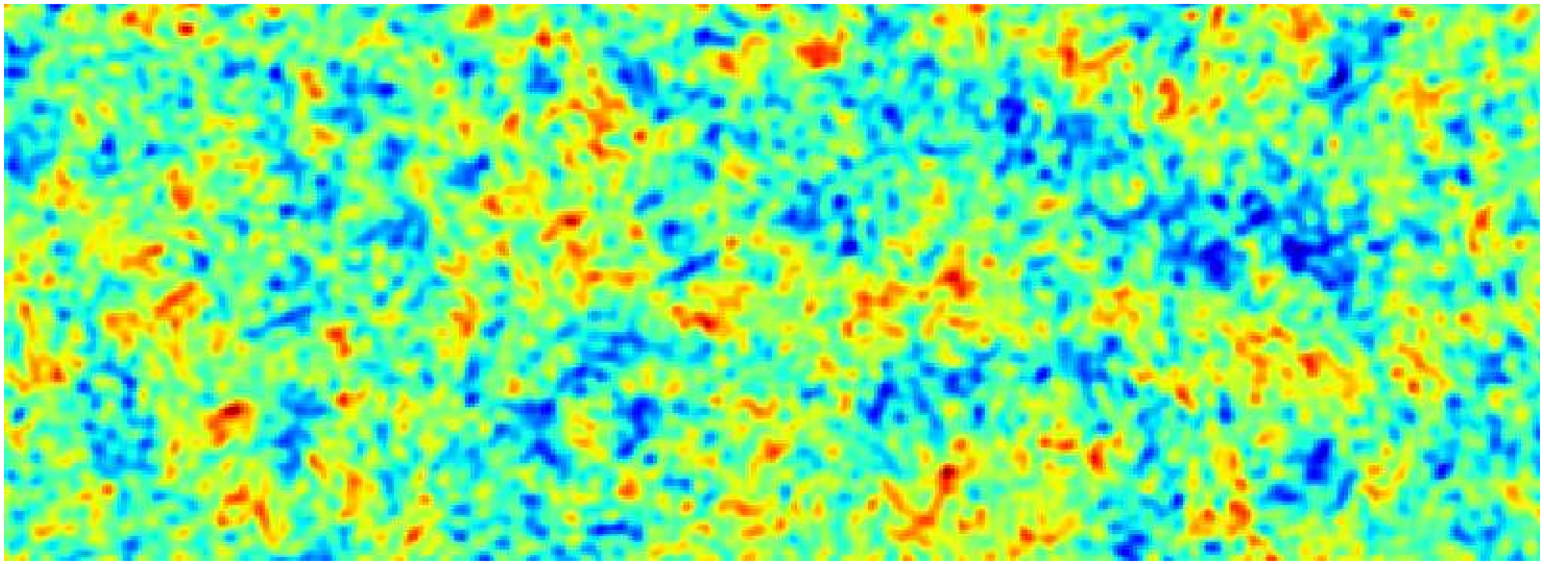

κ

$$C_l^{\kappa g} = \int_0^\infty dz \frac{H(z)}{\chi^2(z)} W_\kappa(z) W_g(z) P\left(\frac{l}{\chi(z)}, z\right)$$

Physics of lensing-galaxy correlation

- Radio galaxies are biased tracers of the underlying dark matter density field
- CMB lensing also due to density fluctuations of the dark matter

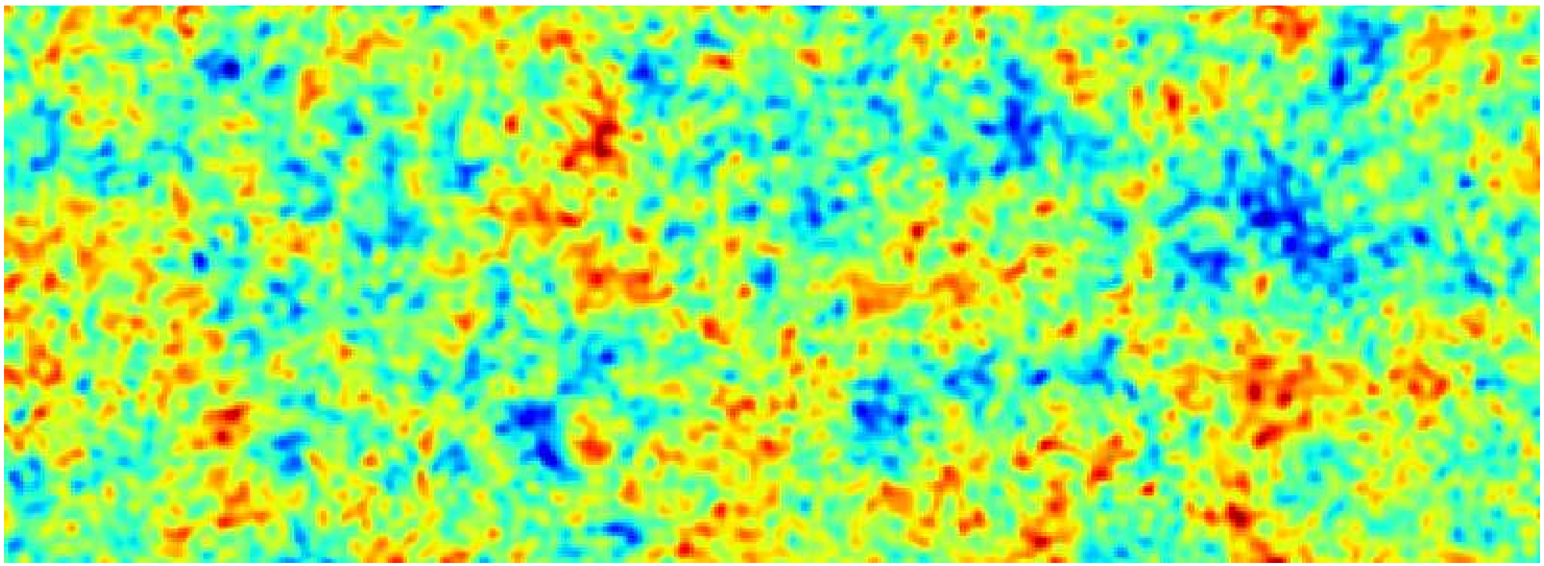

g

$$C_l^{\kappa g} = \int_0^\infty dz \frac{H(z)}{\chi^2(z)} W_\kappa(z) W_g(z) P\left(\frac{l}{\chi(z)}, z\right)$$

Physics of lensing-galaxy correlation

- Radio galaxies are biased tracers of the underlying dark matter density field
- CMB lensing also due to density fluctuations of the dark matter

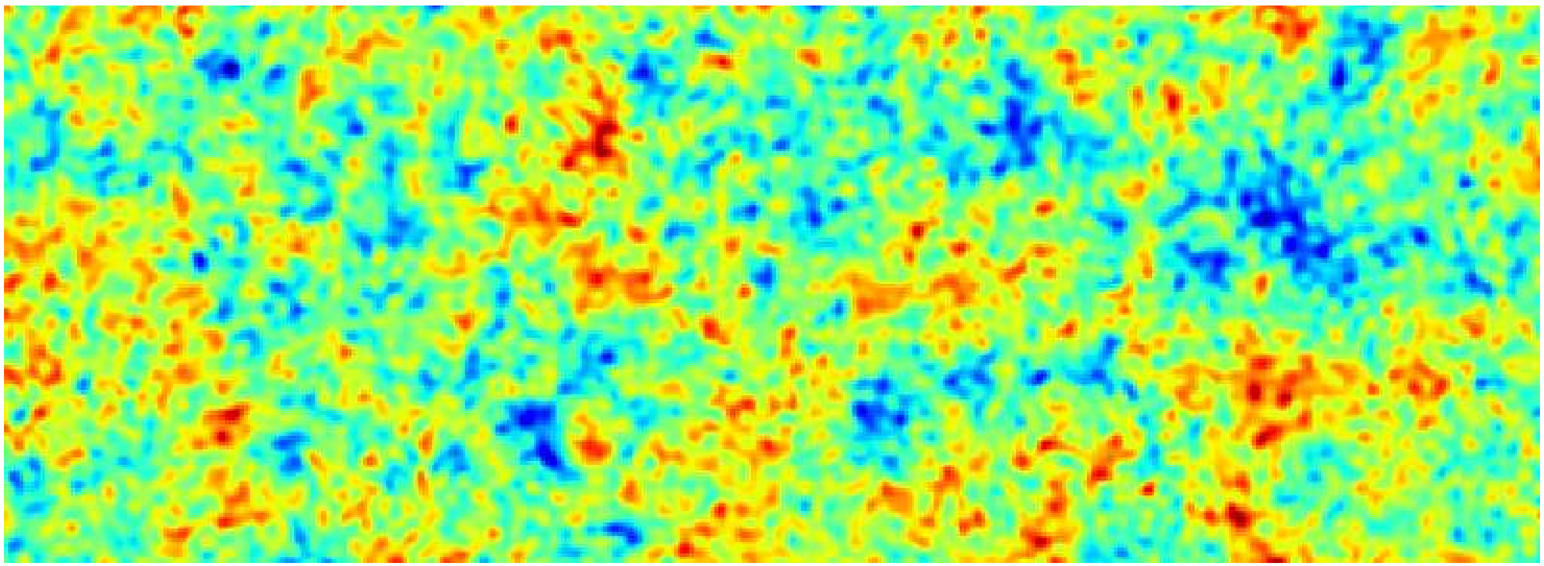

g

$$C_l^{\kappa g} = \int_0^{\infty} dz \frac{H(z)}{\chi^2(z)} W_\kappa(z) W_g(z) P\left(\frac{l}{\chi(z)}, z\right)$$

Window functions

$$W_g(z) \propto b(z)$$

Physics of lensing-galaxy correlation

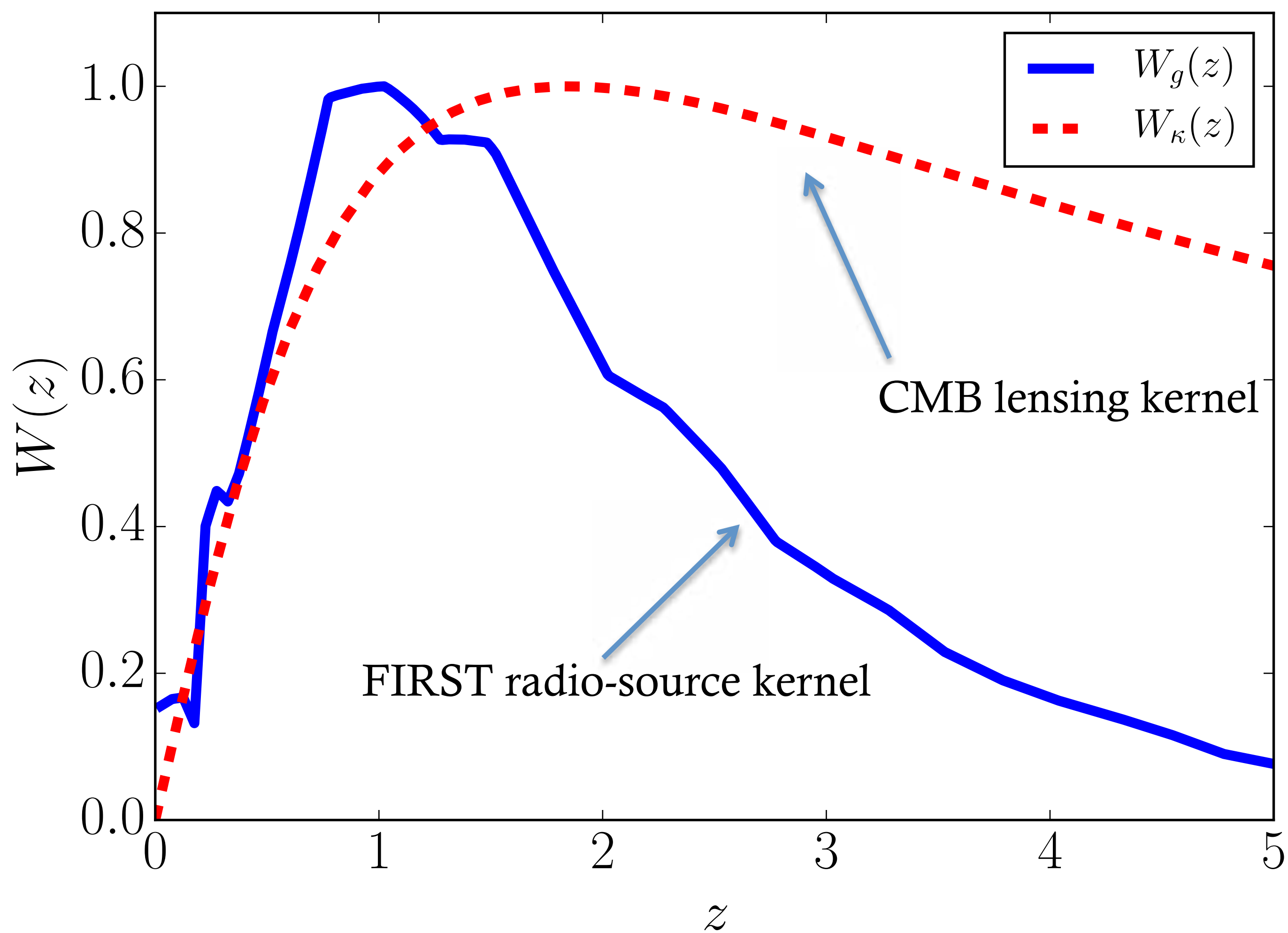

CMB lensing from ACT

Atacama Cosmology Telescope

- Cerro Toco, Northern Chile
- 6m dish CMB telescope
- ACTPol polarimeter fitted 2013
- 90,150 GHz
- First *T* and *P* data in Naess et al. (2014)
- Cross-correlation of lensing with CIB (Van Engelen et al. 2014), detection of CMB lensing 1-halo term (Madhavacheril et al. 2015)

Photo: Lyman Page

CMB lensing from ACTPol

$$\hat{\phi}(\mathbf{L}) = A(\mathbf{L}) \int \frac{d^2\mathbf{l}}{(2\pi)^2} F(\mathbf{l}, \mathbf{L} - \mathbf{l}) T(\mathbf{l}) T(\mathbf{L} - \mathbf{l})$$

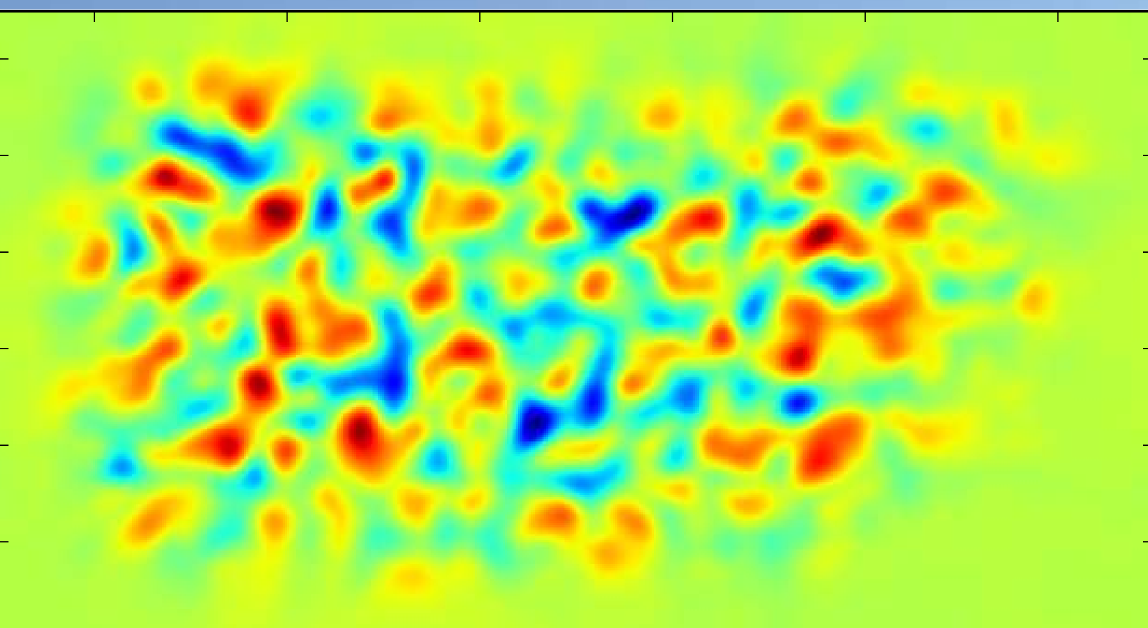

ACTPol D1 convergence

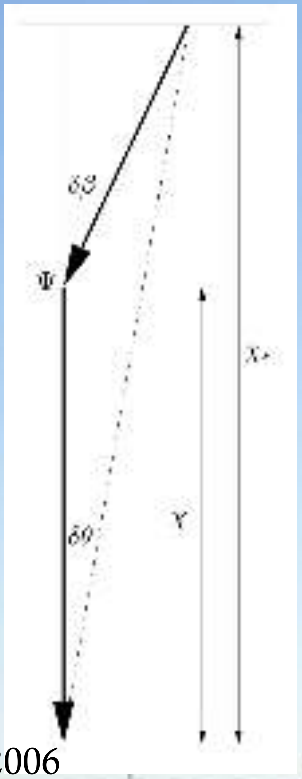

Lewis & Challinor 2006

Planck lensing potential

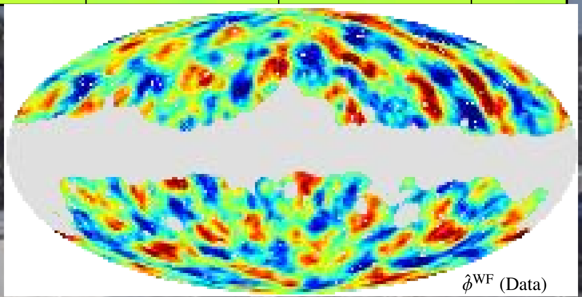

Photo: Lyman Page

FIRST radio survey

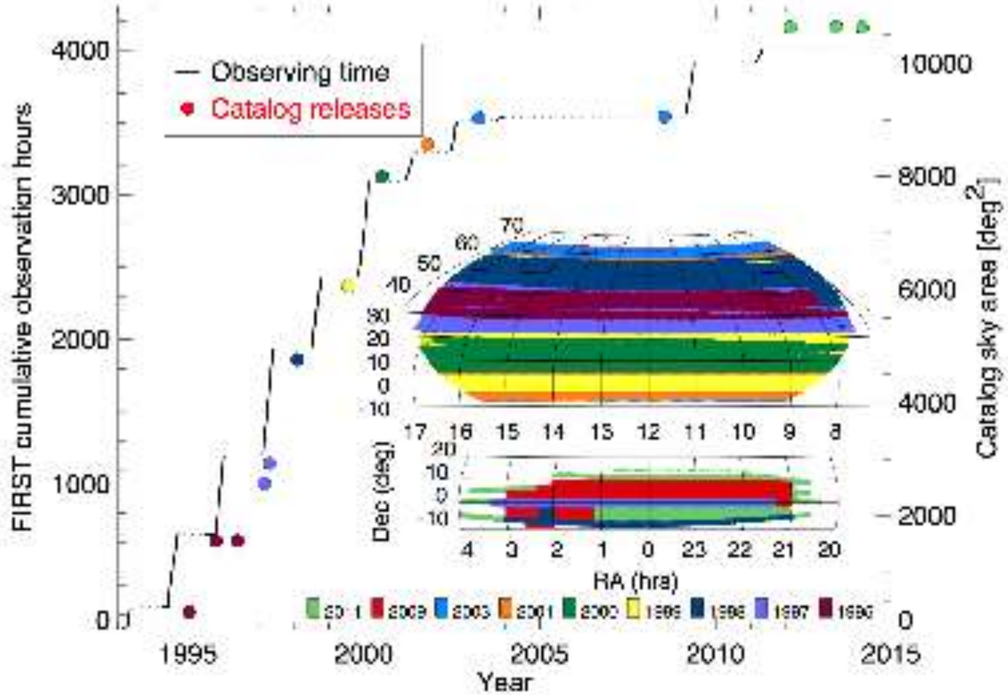

Helfand et al. 2015

- 10,000 sq. deg covered over 20 years (1993-2011), final catalogue 2015.
- 1.4 GHz observing frequency
- 95% complete at 2 mJy
- Around 10^6 sources detected, 720,000 are reliable and have $F_{1.4\ \mathrm{GHz}} > 1\ \mathrm{mJy}$
- Low-redshift sources (z<0.2): dominated by star-forming galaxies
- High-redshift sources (z>0.2): dominated by synchrotron-emitting **AGN**
- Optical cross-matching with SDSS to remove most of the SFGs
- Final sample of sources used in analysis**: 36,000 sources over 500 sq. deg** of ACT and ACTPol lensing coverage

arXiv:1502.06456

Overlap between ACT, ACTPol and FIRST

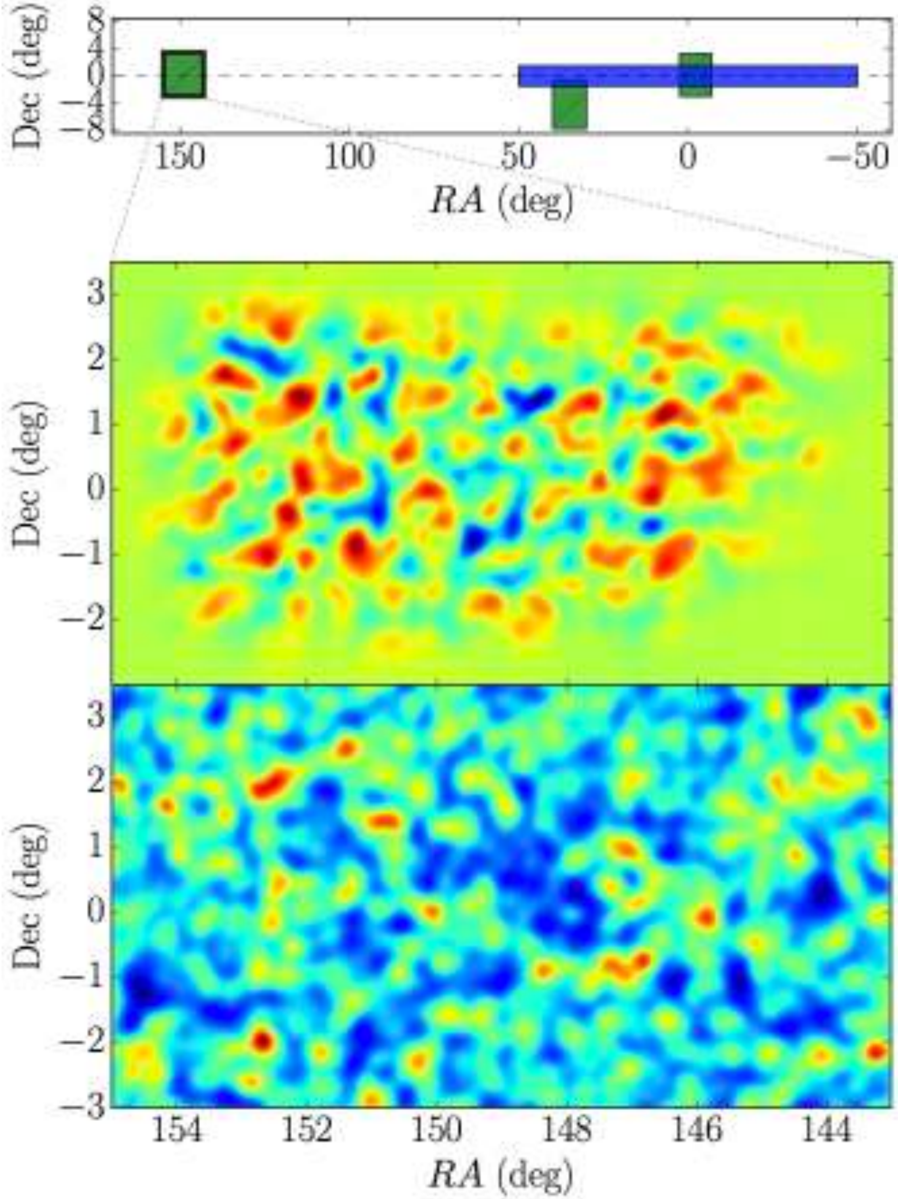

arXiv:1502.06456

Results

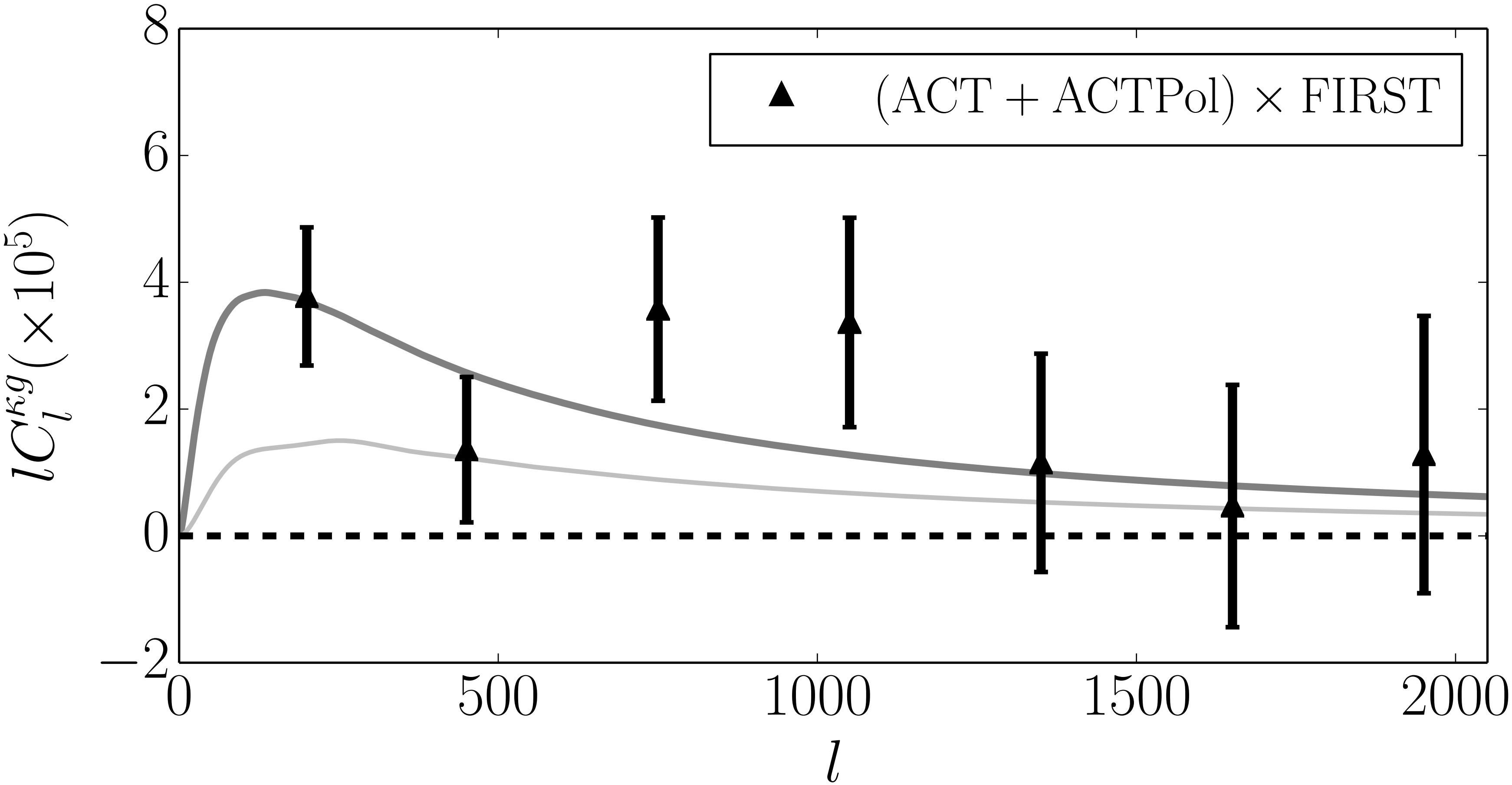

Dark solid: best-fit cross-spectrum

Light solid: contribution to cross-spectrum from $z > 1.5$ sources

4.5σ detection of the cross-spectrum, corresponding to $\sim 2 - 60$ Mpc fluctuations at an effective redshift of $z_{\rm eff} = 1.5$

arXiv:1502.06456

Results

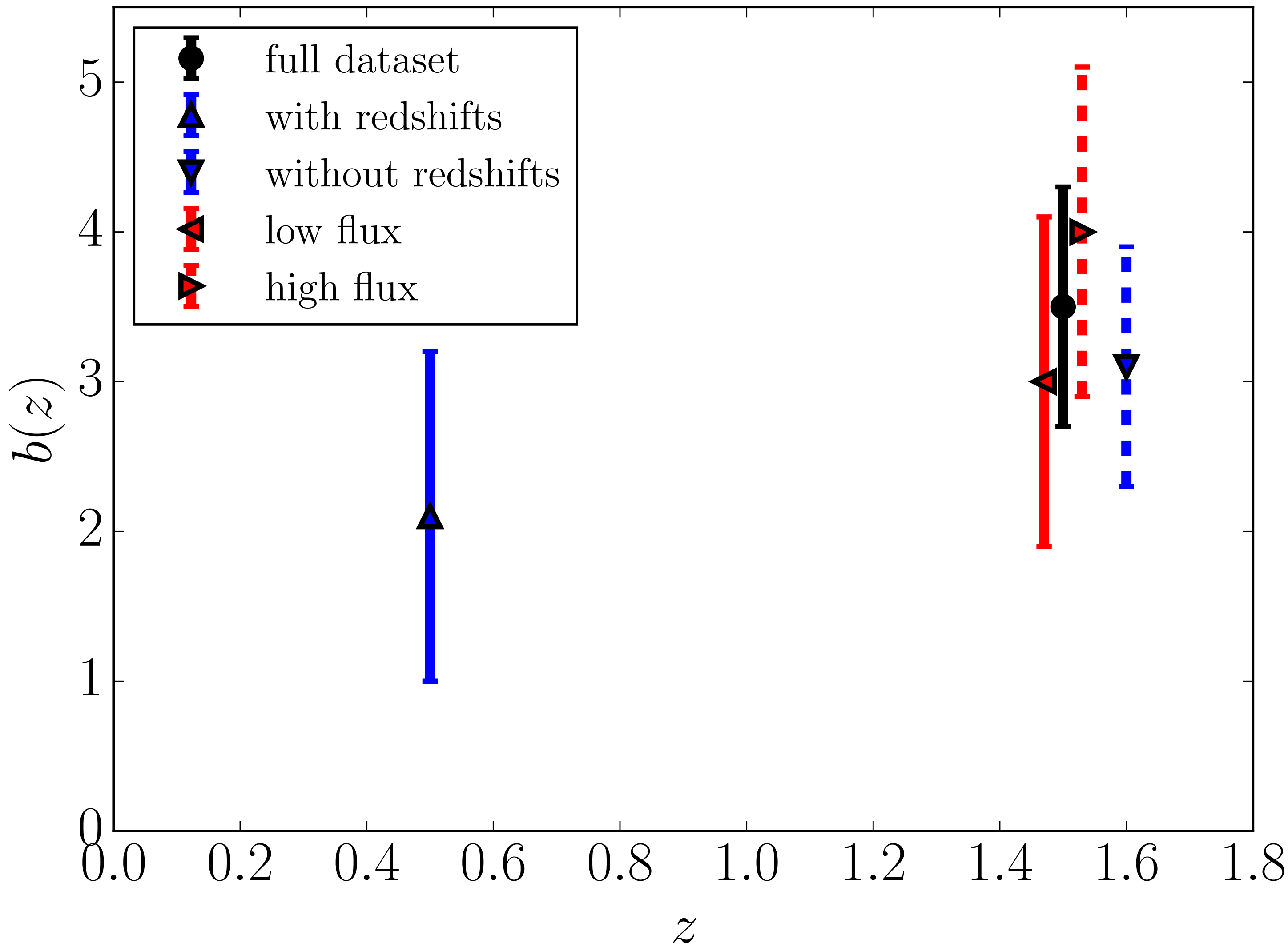

arXiv:1502.06456

Future science with $g, \kappa_{\rm cmb}, \kappa_g$

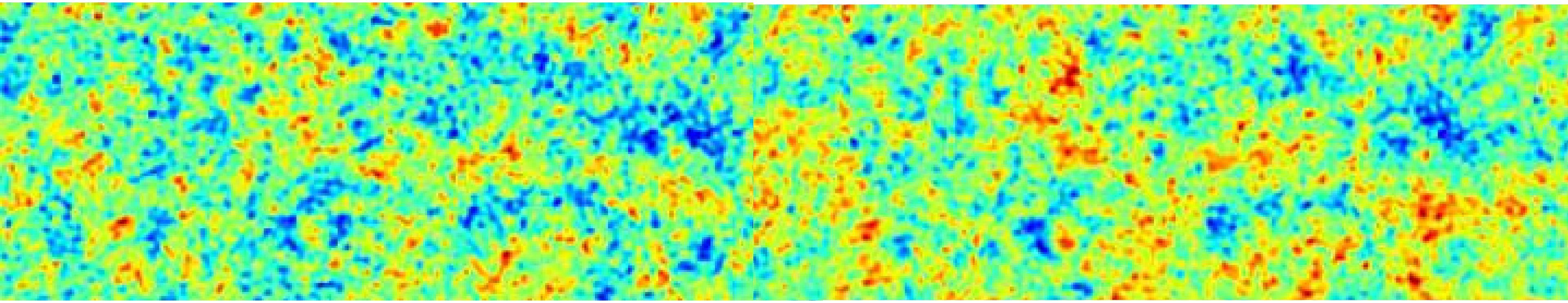

- The auto- and cross-spectra provide complementary information about the large-scale structure they probe.
- Cross-spectrum robust to systematic biases particular to each data set – use as a calibrator
- Kirk et al. (2015) show inclusion of cross-spectra can significantly improve cosmological constraints (probing different structure, suppressing astrophysical degeneracies).
- Next-generation CMB experiments in combination with the SKA will provide sub-percent constraints on the amplitude for WL and LSS cross-correlations with CMB lensing

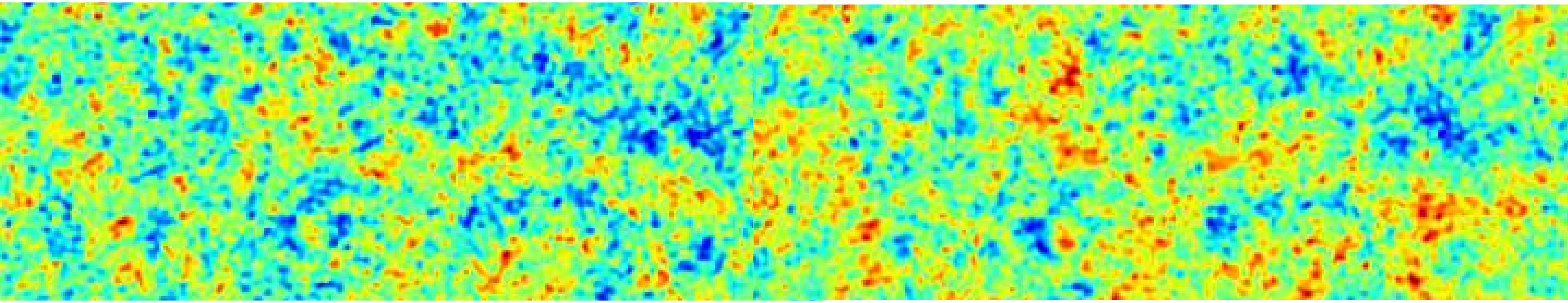

Thanks for listening! Questions?

Bonus slides

Systematics, modeling limitations, z_{eff}

- Previous work shows high-redshift underlying dn/dz most uncertain (e.g. Jarvis & Rawlings 2003, Jarvis+ 2001, Wall+ 2005, Rigby 2011). Perturbing dndz here, only see a 0.25σ shift – expect this to be a subdominant bias.

- Choice of cosmology – fixed to Planck bf; error contribution from model uncertainty negligible.

- Astrophysical contaminants:
  - IR sources, SZ clusters, Galactic cirrus. Ref. to Sherwin et al. (2012).
  - Subtraction of bright radio sources from primary CMB prior to lensing reconstruction.

Effective redshift

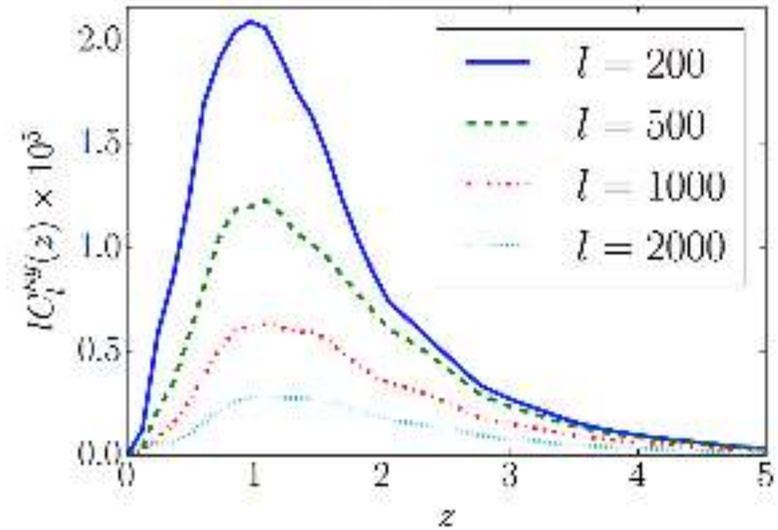

Figure 9. Cross-power spectrum kernel $C_l^{\kappa g}(z) = W_\kappa(z) W_g(z) P(l/\chi(z); z)$, demonstrating the scale-dependent sensitivity of the cross-spectrum to source redshift. At $l = 200$, where the signal-to-noise peaks, the mean redshift of the kernel is $\int z C_{200}^{\kappa g}(z) dz / C_{200}^{\kappa g} = 1.5$, which we adopt as the effective redshift z_{eff} of the radio source bias measurement. The spread in the kernel reflects sensitivity to a wide range of redshift. See Section 2.3 for details.

arXiv:1502.06456

Pipeline verification

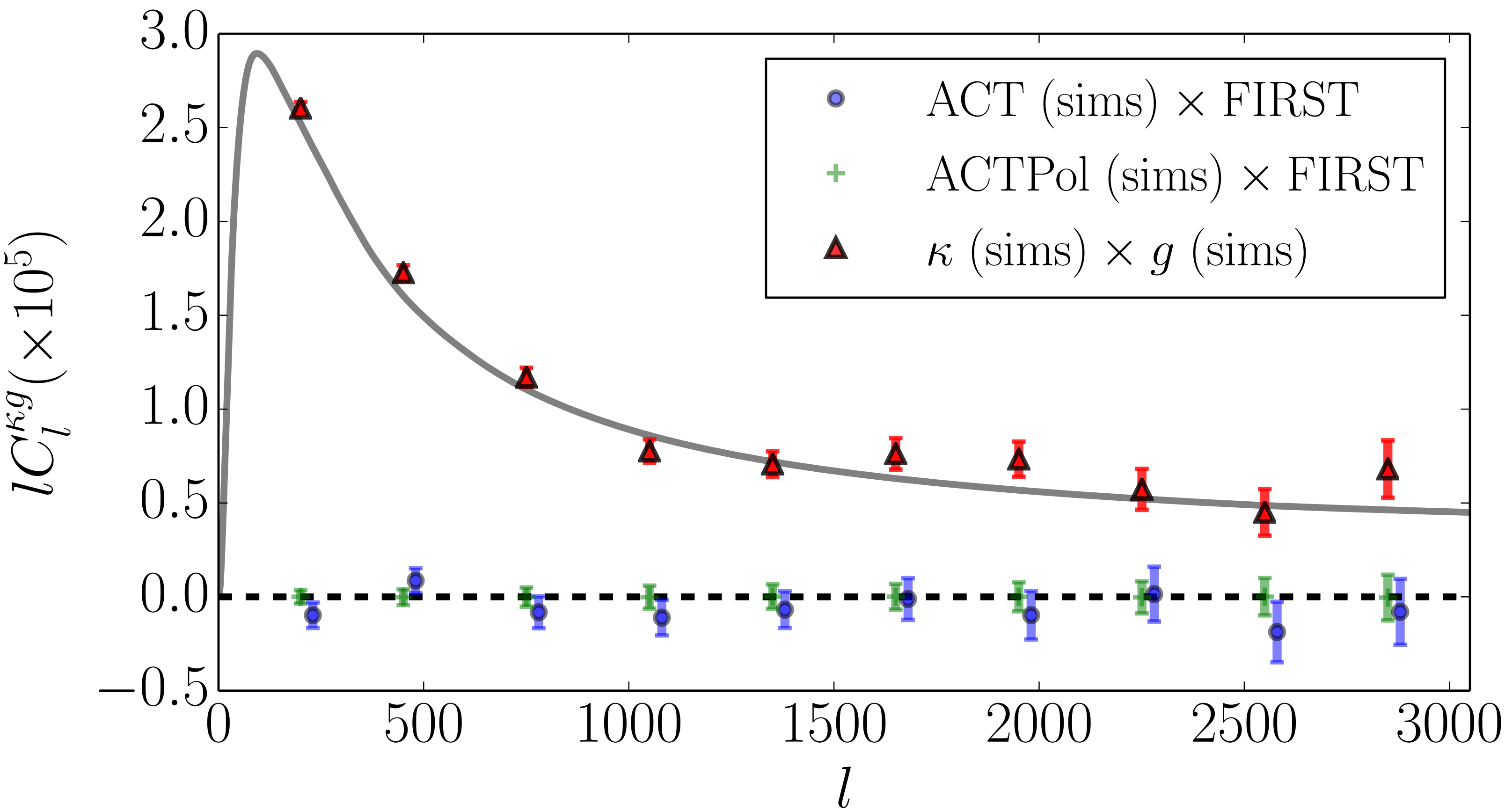

arXiv:1502.06456

ACT × FIRST, ACTPol × FIRST

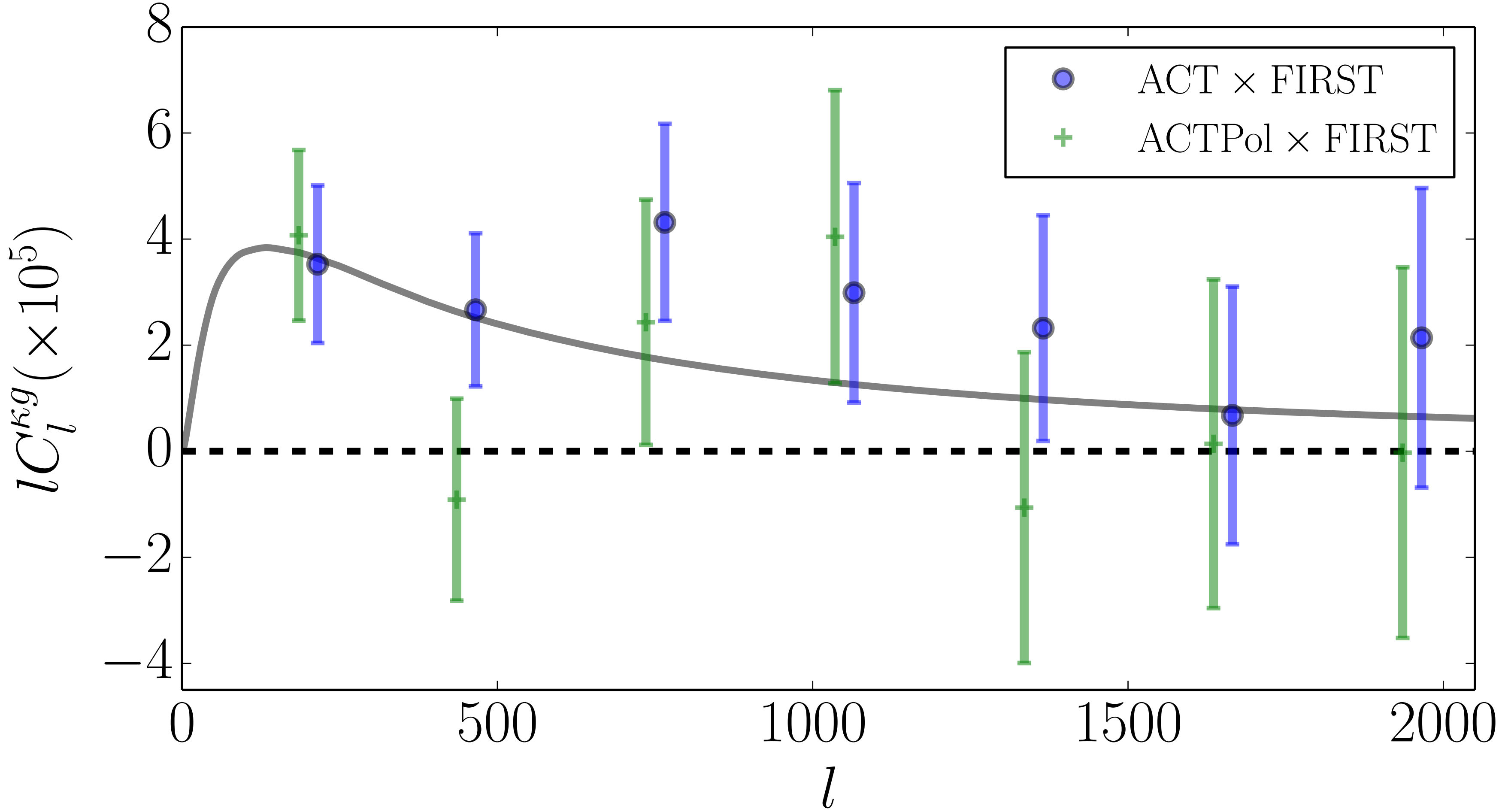

arXiv:1502.06456

Stats

	A	S/N	χ^2 (ν)	PTE
ACT	1.22 ± 0.31	3.9	3.2 (9)	0.96
ACTPol	0.85 ± 0.36	2.4	7.2 (9)	0.62
Comb.	1.06 ± 0.24	4.5	11.0 (19)	0.92

Table 2. Results showing the bias amplitude A relative to the fiducial model of Fig. 3. We also quote the signal-to-noise ratio S/N, Chi-squared values at the best-fit χ^2, the number of degrees of freedom ν and the probability to exceed this χ^2 (PTE) under the assumption of the best-fitting model.

arXiv:1502.06456